Theoretical model of TEA nitrogen laser excited by electric discharge
1. Problem formulation

J. Makuchowski, L. Pokora

Laser Technics Centre, ul. Kasprzaka 29/31, 01−234 Warszawa, Poland.

A computer simulation of the nitrogen laser excited by a transversal electric discharge is presented. This simulation was based on a specially constructed theoretical model of the laser. For these purposes, analysis of the phenomena leading to creation of population inversion was carried out, a list of most important kinetic reactions occurring in the electric discharge in the gaseous nitrogen was made. A set of equations describing the kinetics of the medium has been given. The assumptions and simplifications accepted in the model were justified. The results of this work were compared with the data reported in the available literature. The whole paper has been divided into three parts. The first part is devoted to the problem formulation so far as physical phenomena and the corresponding mathematical equations are concerned. The second part presents the results of calculations and discussion of the latters. The third part contains the description of construction of two nitrogen lasers of TEA type performed by the authors. Also, in this part the selected results of preliminary examinations of one of these lasers are reported.

1. Introduction

Nitrogen lasers generate nanosecond pulses of UV radiation of relatively high power. The most intensive line in the spectrum of radiation emitted by these lasers corresponds to the wavelength $\lambda = 337.1$ nm. High power (of order of single MW) and short duration (from 1 to 20 ns) of the radiation pulses emitted as well as high frequency of repetitions (of order of kHz) are characteristic of nitrogen lasers. These may be achieved, for a relatively simple and reliable construction, without necessity of applying any complicated systems either forming or shortening the pulse.

The variety of processes and phenomena occurring in the active medium of the laser makes the theoretical description a difficult task. On the other hand, the multitude of the external parameters determining the operation of the nitrogen laser causes the experimental examinations of these lasers very laborous and costly. The results obtained are difficult to compare even among slightly little differing practical systems described in the literature [1]−[6]. The mathematical description requires the knowledge of a great number of parameters. The precision of their determination influences the practical usability of the results generated by the accepted model. The performance of the optimal construction of nitrogen laser requires, in general, a due combination of experimental methods and theoretical modelling, both in suitable proportions.

The theoretical models constructed up-to-date, for instance those described in papers [7]−[17], concern selected problems of nitrogen lasers. In these papers, the theoretical description is devoted to a narrowed regime of laser operation. Often, these models deal with some special cases of working conditions for lasers. Consequently, they are not complete and their direct application to design of the practical laser systems can be very difficult and sometimes even impossible. In the literature, the data concerning the characteristics of the active media as well as the pumping systems are most often incomplete. Similarly, in an incomplete and selective way there are given the values of the following parameters: kinetics coefficients, cross-sections in particular processes and also the manner of modelling the of nonlinear discharge circuits. Thus, although the literature descriptions render many possible design solutions, the final result is often uncertain. The attempts to adapt the results of calculations made according to the theoretical models described in the literature to practical model design did not provide the satisfying effects.

The aim of this work was to construct an original and complete theoretical model of nitrogen lasers excited by electric discharge. Such a model should assure a correct choice of parameters for practical design on the one hand and a possibility of easy controlling the selected parameters of radiation by a suitable choise of external parameters on the other hand.

An additional justification of the aim of the paper was that in spite of the fact that the first nitrogen laser was set into operation as early as in 1963 [18], the design of these lasers is still the subject of high interest both from the application and research points of view. Especially interesting and perspective are the applications of these lasers to the cancer diagnostics [19]. Still a broad application exists in such fields as: measurement techniques (ultraspeed photography, interferometry), micro-technology (photoablation, thin film processing, electronic element correction, liothgraphic processes), as well as in many fields of medicine. The fact that in 1975 an excimer laser generating the pulses of radiation of energy twice as high as that of the N_2 lasers caused practically no reduction of interest in the latter. In contrary, an increase of interest is observed in nitrogen lasers somehow connected with the discovery of new, fantastic possibilities of applications of excimer lasers. This is due to the low cost of both production and exploitation of the nitrogen lasers (easy availability of nitrogen). In some fields, especially when high direct energy of UV radiation in nanosecond pulse is desired, the nitrogen lasers compete successfully with both excimer lasers and the third harmonic of the YAG:Nd lasers.

2. General characteristics of the model

A correct description of the phenomena occurring during the electric discharge in nitrogen requires the knowledge of the molecule structure and the possible quantum transitions connected with this molecule. Especially important is the knowledge of the kinetics of the processes, reaction rate coefficient and the cross-sections involved in stimulation of the inversion in the active medium.

The excitation of the nitrogen laser medium is mostly achieved by electric discharge. It is realized in the LC circuits with overcharged capacity or in the systems with pulse-forming line. As the results of many experimental examinations [13], approximate values of characteristic discharge parameters were determined, *i.e.*:
— current density in the laser chamber equal to about 10^4 A/cm^2,
— rate of current increase in the laser chamber equal to about 10^{12} A/s,
— optimal value of E/p ranging from 100 to 180 V/cm h Pa (E — strength of the electric field between the electrodes of the laser chamber, p — pressure of nitrogen).

These requirements may be satisfied by an electric circuit of the laser of correctly chosen parameters.
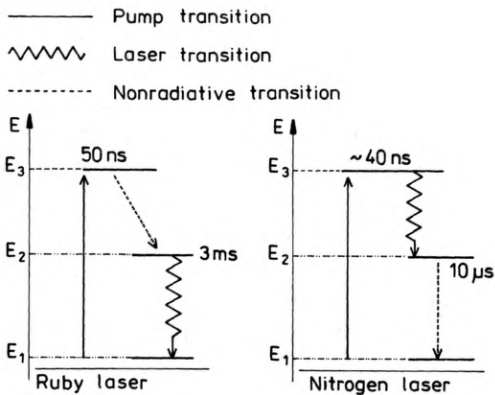

Fig. 1. Comparison of three-level quantum systems of ruby and nitrogen lasers

Let us compare the sets of energy levels of N_2 molecule and chromium ion being the active material of the classic ruby laser both shown in Fig. 1. The excited state E_3 is short-lived (average lifetime about 50 ns), while E_2 is metastable, its lifetime being of the order of 3 ms. Being excited by light the level 3 becomes populated. The direct return of the ion to the basic state is little probable. Between the short-lived level 3 and metastable level 2 non-radiant transition occurs * and next — after average time of order of few millisecond — the radiant transition of $2 \rightarrow 1$ type is realized. In the N_2 molecule, the situation is totally different. The same quantum system being preserved, the radiant transition occurs between the levels E_3 (short-lived — 40 ns) and the metastable E_2 (lifetime — 10 ns). In order to produce their inversion for such a big difference in lifetimes of the laser levels, a very strong and very quick pumping of the upper laser level is needed which is realized by strong current discharge in the gas or a beam of high-energy particles [1], [21]. An untypical (for a lasing medium) set of the energy transitions in the nitrogen molecules, between which a radiative transition occurs in the UV region, is the reason of complexity of the theoretical description of the nitrogen laser.

---

* The energy difference $E_3 - E_2$ is transferred to the medium causing its heating.

In the nitrogen molecule, the short lifetime of the upper energy level E_3, as compared to the lower one E_2, enables the generation of radiation pulses only of duration of order of single nonoseconds. The pulse duration depends strongly on the gas pressure. Short radiative lifetime of the upper laser level E_3 causes its quick emptying in the form of stimulated emision. Hence there is no possibility of forming a laser beam in the nitrogen laser in the way analogous to that in classical resonators and the emission of energy occurs in the form of superradiation [1].

A detailed set of energy levels for the nitrogen molecule will be presented in the further part of this work.

2.1. Properties of N_2 molecule

In order to formulate a theoretical model of the N_2 laser a good knowledge of quantum-mechanical properties of the nitrogen molecule is very helpful. This molecule being of monomolecular type posseses both axis and centre of symmetry and a plane of reflection. This determines the set of electron energy states, the degree of their degeneration and the possible optical transitions between them. The potential curves for more important electron states, depending on the inter-nucleus distance, are shown in Fig. 2. The meaning of the quantum numbers, terminology and the conservation laws may be found in [22], for example.

As it has been shown in Figure 2, the state of the lowest energy is the state $X^3\Sigma'_g$. This is the basic state and it is denoted by X. The state $A^3\Sigma_u^+$ is located about 6.2 eV above the basic state. This state is denoted by A. The next electron state of the
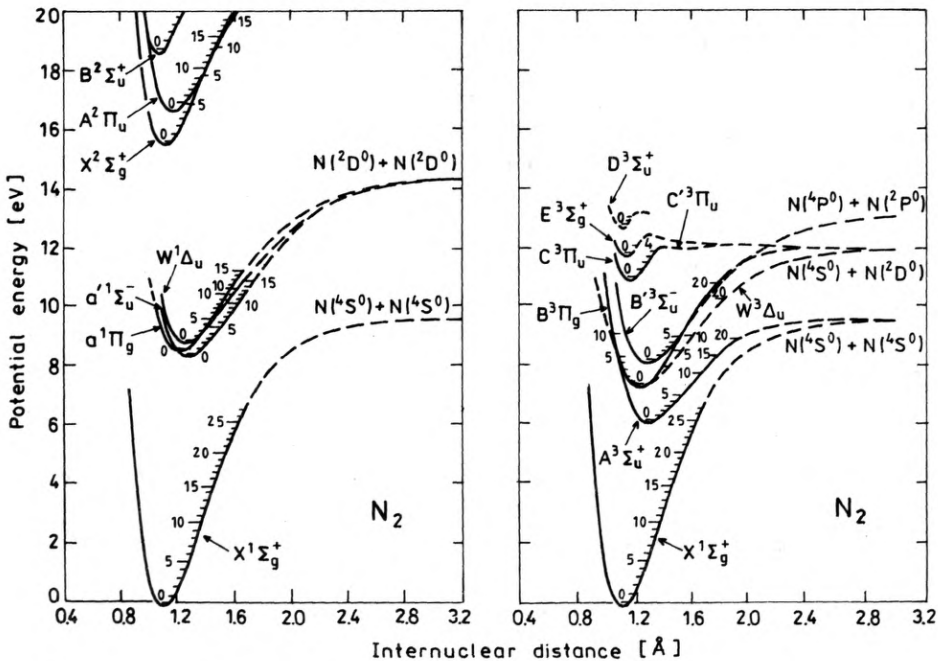

Fig. 2. Diagrams of potential energy of N_2 molecules [1]

N_2 molecule is the state $B^3 \Pi_g$ which is denoted by B. It is located about 7.2 eV above the state X. The state A plays an essential role in its depopulation [23]. Both the states A and B are metastable states. The state $C^3 \Pi_u$ lying about 10.9 eV above the state X is denoted by C. The radiative transitions in the ultraviolet range (UV) in the N_2 molecule take place between the state C (the upper laser level) and the state B (the lower laser level). Both the states lie in the symmetric (positive) branch of the N_2 electron states. From the energy difference in the minima of the respective potential curves of the states C and B, it follows that the shortest wavelength possible to achieve in this system is equal to $\lambda = 337.13$ nm. From the symmetry principle of the N_2 molecule, it follows that the direct transition from the basis state X to the state B is forbidden which allows us to achieve inversion of population between the states C and B, while the direct excitation from the basic state occurs, if a sufficiently quick pumping is applied. The lifetime of the level C is given by the formula [24]

$$\tau_c = \frac{36}{1 + 0.0129352p} \; [\text{ns}] \tag{1}$$

where p — pressure, in hPa.

On the other hand, the natural lifetime of the level B amounts to ca. 10 µs [11]. The lifetime τ_c diminishes with the increase of the pressure causing a reduction of amplification in the spectrum line and as a consequence both the lifetime and the laser generation power become reduced. If it is assumed that the populating of the laser levels C and B occurs as a result of excitation from the basic state, the essential part is played by the ratio of effective cross-sections of the excitation of electron levels. The total cross-section for excitation of the state C is less than that of the state B, which, in turn, is less than that for the state A. Under such circumstances the population inversion may take place only for some oscillating states.

The subsequent oscillating states v of electrons are marked in the potential curves. Theoretically, there is infinitive number of them. In practice the observed transitions are those from the oscillating states of quantum numbers $v = 0, 1, 2$ [12]. The transition $C \rightarrow B$, $\lambda = 337.1$ nm, being most intensive [25] is a transition of type $n' \rightarrow n''$, $v' = 0$ and $v'' = 0$. Besides, the transitions $v' = 0, 1, 2, 3 \rightarrow v'' = 0$, $v' = 0, 1, 2 \rightarrow v'' = 1$ and $v' = 0 \rightarrow v'' = 0, 1, 2$ are observed. The electron state B of oscillation number $v'' = 0$ is marked by $B0$. On the other hand, when the oscillation number $v'' = 1$, the due state is denoted by $B1$. According to paper [26], the ratio of the number of particles in the states $B1$ and $B0$ during the electric discharge is 1:50. For the given transition, the subsequent wavelengths are located in three branches — longwave branch P, branch Q, shortwave branch R. The branch Q is twice weaker than P and R and almost does not appear at all.

The knowledge of the properties of the nitrogen molecule described above allows us to formulate the kinematic equations of the medium.

2.2. Kinetic equations

Many complex channels of energy transfer lead from the initial excitation of the gas molecules (due to pumping) to the extraction of laser radiation in gas lasers.

In the nitrogen laser they are realized under the influence of the electric discharge due to processes of ionization and excitation as well as to two- and three-particle collision process. The model of time evolution of such a system must define and determine quantitatively the concentration of great number of particles, typically between 20 and 60, taking account of both ground and excited states of ions, atoms and molecules as well as the electrons and photons.

A common difficulty in construction of all kinetic models of nitrogen lasers is to formulate the list of the essential reactions with the reliable rate coefficients. The rate of the reactions is decisive for its significance. However, for many reactions their rates are not uniquely determined. For the majority of them, the coefficients obtained in measurements are known but some values differ by an order of magnitude. There occur also such reactions, the coefficients of which are estimated by analogy to the similar ones.

In the kinetic equations, the coefficients of the reaction rate k_r are used. In order to calculate them the knowledge of the electron energy distribution function is necessary in addition to the value of the cross-section for a given reaction. Similarly to [27], the Maxwell-type distribution was here assumed. A broader justification of this assumption will be present in Section 3 of this paper. The rate coefficients for nonelastic collisions (the reaction rate coefficients) between particles and electrons have the form

$$k_r(\varepsilon) = \left[\frac{2}{m}\right]^{1/2} \int_0^{\infty} \sigma_r(\varepsilon)\varepsilon^{1/2} f(\varepsilon, \overline{\varepsilon}) \, d\varepsilon \tag{2}$$

where: σ_r — cross-section for a given process,
   ε — electron energy,
   m — electron mass,
   f — electron energy distribution function normalized as follows:

$$\int f(\varepsilon) d\varepsilon = 1.$$

The most essential channal of creation of particles in the excited state $N_2(C^3\Pi_u, v' = 0)$, which is the upper laser state for emission in the UV band ($\lambda = 337.13$ nm), is the direct collision of the nitrogen molecules with electrons according to reaction

$$N_2(X^1\Sigma_g^+) + \tilde{e}^* \rightarrow N_2(C^3\Pi_u, v' = 0) + e. \tag{3}$$

The rate of this reaction is a function of the cross-section and the electron velocity and has been calculated according to the formula presented above. The upper laser level is attenuated in two main reactions. These are, firstly, the reaction with nitrogen particles:

---

* $E(\tilde{e}) > E(e)$.

$$N_2(C^3\Pi_u, v=0)+N_2 \left\{ \begin{array}{l} \overset{42^*}{\to} N_2(B0)+N_2, \\ \overset{43}{\to} N_2(B1)+N_2, \\ \overset{41}{\to} N_2+N_2, \end{array} \right. \tag{4}$$
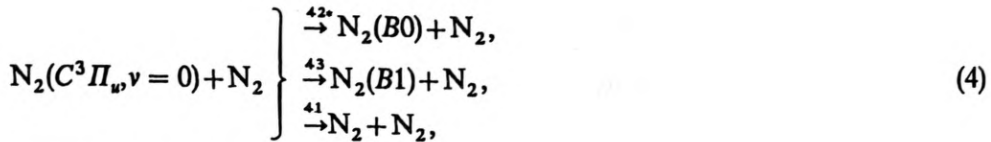
and, secondly, collision with electrons:
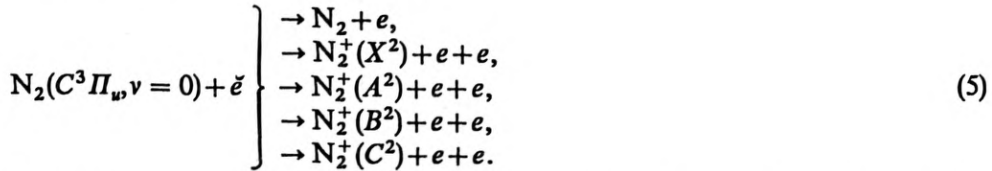
$$N_2(C^3\Pi_u, v=0)+\breve{e} \left\{ \begin{array}{l} \to N_2+e, \\ \to N_2^+(X^2)+e+e, \\ \to N_2^+(A^2)+e+e, \\ \to N_2^+(B^2)+e+e, \\ \to N_2^+(C^2)+e+e. \end{array} \right. \tag{5}$$

The greatest contribution to creation of the state $B^3\Pi_g$, $v=0$ is given by the collision reaction of electron with nitrogen molecules being in basic state

$$N_2(X^1)+\breve{e} \to N_2(B0)+e. \tag{6}$$

Depopulation of the excited nitrogen molecules in the state $B0$ occurs in the collision reactions:

$$N_2(B0)+N_2 \left\{ \begin{array}{l} \overset{1}{\to} N_2(A^3)+N_2, \\ \overset{4}{\to} N_2+N_2, \end{array} \right. \tag{7}$$

$$N_2(B0)+\breve{e} \left\{ \begin{array}{l} \to N_2^+(A^2)+e+e, \\ \to N_2^+(B^2)+e+e, \\ \to N_2^+(C^2)+e+e. \end{array} \right. \tag{8}$$

As a result of the analysis of the nitrogen gas lasing medium, the following atomic and molecular states (denoted below by symbol N_i) have been taken into account: $N_2(X^1\Sigma_g^+)$, $N_2(A^3\Sigma_g^+)$, $N_2(B^3\Pi_g, v=0)$ — lower laser level, $N_2(B^3\Pi_g, v=1)$, $N_2(a'^1\Sigma_u^-)$, $N_2(a^1\Pi_g)$, $N_2(C^3\Pi_u, v=0)$ — upper laser level, $N_2^+(X^2\Sigma_g)$, $N_2^+(A^2\Pi_u)$, $N_2^+(B^2\Sigma_u^+)$, $N_2^+(C^2\Sigma_u^+)$, N^+, N_4^+, N_3^+. By the same means the laser medium has been described by the set of 14 levels. In Figure 3, the set of electron levels with marked reactions has been presented. The above list of states is completed by electrons and photons. Above 70 reactions occurring between these states are taken into account. The list of reactions and the coefficients of their rates are shown in the Table.

The kinetic equations are of general form

$$\frac{dN_i}{dt} = \sum_r \Delta_{ir} k_r \bigcap_{j=1}^n N_{jr} \tag{9}$$

where: Δ_{ir} — difference of quantity on the right and left sides of i-th particle in reaction r,

---

* These indexes correspond to the reaction number in the Table.

k_r — kinetics coefficient dependent on electron energy,
N_{jr} — concentration of particles taking part in reaction r,
n — number of particles taking part in reaction $n(r) = 1, 2, 3 \dots$.

Fig. 3. Set of electron levels of nitrogen molecule with marked reactions and collision transitions

An exemplified kinetics reaction for a particle $N_i = N_2^+(B^2\Sigma_u^+)$ arranged on the basis of the Table while taking account of the value of parameter $\Delta_{ir} (= 0, -1, 1)$ has the form

$$
\begin{aligned}
\frac{d[N_2^+(B^2\Sigma_u^+)]}{dt} =\ & [N_2^+(X^2)][N_E]k_{24} + [N_2^+(B^2)][N_E]k_{26} \\
& - [N_2^+(B^2)][N_E]k_{28} + [N_2(X)][N_E]k_{31} \\
& + [N_2(A^3)][N_E]k_{35} + [N_2(B^3)][N_E]k_{45} \\
& + [N_2(C^3)][N_E]k_{49} + [N_2(a'^1)][N_E]k_{53} \\
& + [N_2(a^1)][N_E]k_{57} - [N_2^+(B^2)][N_E]k_{68}
\end{aligned}
\tag{10}
$$

where [ ] denotes the concentration of the component included inside the brackets. The time evolution of the electron concentration N_E is described by the equation

$$
\frac{dN_E}{dt} = \sum_r \Delta_r k_r \bigcap_{j=1}^{n} N_{jr}
\tag{11}
$$

where: Δ_r — difference in number of electrons after and before reaction.

The change of the average electron energy $\bar{\varepsilon}$ may be determined from the equation

$$\frac{d}{dt}[\overline{\varepsilon}\, N_{\mathrm{E}}] = F_1(t) + F_2(t) + F_3(t) \qquad (12)$$

where the particular components are expressed by the formulae:
— contribution from the electric field

$$F_1(t) = \mu N_{\mathrm{E}}\left[\frac{U_{\mathrm{ch}}}{d_{\mathrm{ch}}}\right]^2 e, \qquad (13)$$

— contribution from the elastic collisions

$$F_2(t) = \left[\frac{2}{m}\right]^{1/2} N_{\mathrm{E}} \int \frac{2m}{M} N Q_z \left[\varepsilon^{3/2} f(\varepsilon, \overline{\varepsilon}) + k T \varepsilon^2 \frac{d}{d\varepsilon}[\varepsilon^{-1/2} f(\varepsilon, \overline{\varepsilon})]\right] d\varepsilon, \qquad (14)$$

— contribution from the collision processes

$$F_3(t) = N_{\mathrm{E}} \sum_r S_r(\overline{\varepsilon}) N_r. \qquad (15)$$

In the above formulae, the transport coefficients $S_r(e)$ and $\mu(e)$ appear, being described by the respective formulae:

$$S_r(\overline{\varepsilon}) = \left[\frac{2}{m}\right]^{1/2} \int_0^\infty \sigma_r(\varepsilon) \Delta \varepsilon \varepsilon^{1/2} f(\varepsilon, \overline{\varepsilon}) d\varepsilon, \qquad (16)$$

$$\mu(\overline{\varepsilon}) = \frac{1}{3}\left[\frac{2}{m}\right]^{1/2} \int_0^\infty \frac{e\varepsilon}{N Q_z} \frac{d}{d\varepsilon}[\varepsilon^{-1/2} f(\varepsilon, \overline{\varepsilon})] d\varepsilon \qquad (17)$$

where: N — total concentration of gas,
$\quad\quad N_r$ — concentration of component taking part in the reaction r,
$\quad\quad Q_z$ — cross-section for elastic collisions,
$\quad\quad \overline{\varepsilon}$ — average energy of electrons,
$\quad\quad \Delta\varepsilon$ — change of electron energy during collision,
$\quad\quad U_{\mathrm{ch}}$ — interelectrode voltage,
$\quad\quad d_{\mathrm{ch}}$ — interelectrode distance,
$\quad\quad M$ — atomic mass of gass.

To the above kinetic equations completed by the equation for average electron energy, the equations describing the electric system and the laser radiation should be added. This problems will be the subject of analysis of the consecutive sections.

T a b l e. List of more important collision reactions in the nitrogen laser excited by electric discharge

Number	Reaction	Coefficient of reaction rate	Reference
1	2	3	4
1	$N_2(B0) + N_2 \rightarrow N_2(A^3) + N_2$	1.8×10^{-12} cm^3/s	[26]
2	$N_2(B1) + N_2 \rightarrow N_2(A^3) + N_2$	2.9×10^{-12} cm^3/s	[16]
3	$N_2(B^3) \rightarrow h\nu_1 + N_2(A^3)$	1.1×10^5 s^{-1}	[17]
4	$N_2(B^3) + N_2 \rightarrow N_2 + N_2$	2.25×10^{-12} cm^3/s	[28]
5	$N_2(B^3) \rightarrow h\nu_3 + N_2$	10^6 s^{-1}	[16]

continued

1	2	3	4
6	$N_2(X^1) + \check{e} \rightarrow N_2(A^3) + e$		
7	$N_2(X^1) + \check{e} \rightarrow N_2(B0) + e$		
8	$N_2(X^1) + \check{e} \rightarrow N_2(B1) + e$		
9	$N_2(X^1) + \check{e} \rightarrow N_2(C^3) + e$		
10	$N_2(X^1) + \check{e} \rightarrow N_2(a'^1) + e$		
11	$N_2(X^1) + \check{e} \rightarrow N_2(a^1) + e$		
12	$N_2(B^3) + \check{e} \rightarrow N_2(a'^1) + e$	Coefficients have been calculated	
13	$N_2(B^3) + \check{e} \rightarrow N_2(a^1) + e$	according to formula (2)	
14	$N_2(B^3) + \check{e} \rightarrow N_2(C^3) + e$		
15	$N_2(A^3) + \check{e} \rightarrow N_2(B^3) + e$		
16	$N_2(A^3) + \check{e} \rightarrow N_2(a'^1) + e$		
17	$N_2(A^3) + \check{e} \rightarrow N_2(a^1) + e$		
18	$N_2(A^3) + \check{e} \rightarrow N_2(C^3) + e$		
19	$N_2(A^3) + N_2(A^3) \rightarrow N_2(C^3) + N_2$	1.1×10^{-9} cm^3/s	[16]
20	$N_2(a'^1) + \check{e} \rightarrow N_2(a^1) + e$		
21	$N_2(a'^1) + \check{e} \rightarrow N_2(C^3) + e$		
22	$N_2(a^1) + \check{e} \rightarrow N_2(C^3) + e$		
23	$N_2^+(X^3) + \check{e} \rightarrow N_2^+(A^2) + e$		
24	$N_2^+(X^2) + \check{e} \rightarrow N_2^+(B^2) + e$		
25	$N_2^+(X^2) + \check{e} \rightarrow N_2^+(C^2) + e$		
26	$N_2^+(A^2) + \check{e} \rightarrow N_2^+(B^2) + e$		
27	$N_2^+(A^2) + \check{e} \rightarrow N_2^+(C^2) + e$		
28	$N_2^+(B^2) + \check{e} \rightarrow N_2^+(C^2) + e$	Coefficients have been calculated	
29	$N_2(X^1) + \check{e} \rightarrow N_2^+(X^2) + e + e$	according to formula (2)	
30	$N_2(X^1) + \check{e} \rightarrow N_2^+(A^2) + e + e$		
31	$N_2(X^1) + \check{e} \rightarrow N_2^+(B^2) + e + e$		
32	$N_2(X^1) + \check{e} \rightarrow N_2^+(C^2) + e + e$		
33	$N_2(A^3) + \check{e} \rightarrow N_2^+(X^2) + e + e$		
34	$N_2(A^3) + \check{e} \rightarrow N_2^+(A^2) + e + e$		
35	$N_2(A^3) + \check{e} \rightarrow N_2^+(B^2) + e + e$		
36	$N_2(A^3) + \check{e} \rightarrow N_2^+(C^2) + e + e$		
37	$N_2(B^3) + \check{e} \rightarrow N_2^+(X^2) + e + e$		
38	$N_2(C^3) \rightarrow N_2(B0) + h\nu_L$	2.8×10^7 s^{-1}	[29]
39	$N_2(C^3) \rightarrow N_2(B1) + h\nu_2$	8.6×10^6 s^{-1}	[16]
40	$N_2(C^3) + h\nu_L \rightarrow N_2(B^3) + h\nu_L + h\nu_L$	7.3×10^{-16} cm^2	[25]
41	$N_2(C^3) + N_2 \rightarrow N_2 + N_2$	1.15×10^{-11} cm^3/s	[29]
42	$N_2(C^3) + N_2 \rightarrow N_2(B0) + N_2$	1.65×10^{-11} cm^3/s	[30]
43	$N_2(C^3) + N_2 \rightarrow N_2(B1) + N_2$	2.2×10^{-13} cm^3/s	[16]
44	$N_2(B^3) + \check{e} \rightarrow N_2^+(A^2) + e + e$		
45	$N_2(B^3) + \check{e} \rightarrow N_2^+(B^2) + e + e$		
46	$N_2(B^3) + \check{e} \rightarrow N_2^+(C^2) + e + e$		
47	$N_2(C^3) + \check{e} \rightarrow N_2^+(X^2) + e + e$	Coefficients have been calculated	
48	$N_2(C^3) + \check{e} \rightarrow N_2^+(A^2) + e + e$	according to formula (2)	
49	$N_2(C^3) + \check{e} \rightarrow N_2^+(B^2) + e + e$		
50	$N_2(C^3) + \check{e} \rightarrow N_2^+(C^2) + e + e$		

continued

1	2	3	4
51	$N_2(a'^1)+\check{e} \rightarrow N_2^+(X^2)+e+e$		
52	$N_2(a'^1)+\check{e} \rightarrow N_2^+(A^2)+e+e$		
53	$N_2(a'^1)+\check{e} \rightarrow N_2^+(B^2)+e+e$		
54	$N_2(a'^1)+\check{e} \rightarrow N_2^+(C^2)+e+e$		
55	$N_2(a^1)+\check{e} \rightarrow N_2^+(X^2)+e+e$	Coefficients have been calculated according to formula (2)	
56	$N_2(a^1)+\check{e} \rightarrow N_2^+(A^2)+e+e$		
57	$N_2(a^1)+\check{e} \rightarrow N_2^+(B^2)+e+e$		
58	$N_2(a^1)+\check{e} \rightarrow N_2^+(C^2)+e+e$		
59	$N+\check{e} \rightarrow N^++e+e$		
60	$N^++e+N_2 \rightarrow N+N_2$	10^{-25} cm^6/s	[29]
61	$N^++N \rightarrow N_2^+(X^2)+h\nu_4$	3×10^{-17} cm^3/s	[29]
62	$N_2^+(X^2)+N_2+N_2 \rightarrow N_4^++N_2$	7.2×10^{-29} cm^6/s	[26]
63	$N^++N_2+N_2 \rightarrow N_3^++N_2$	1.8×10^{-29} cm^6/s	[26]
64	$N_4^++e \rightarrow N_2(B^3)+N_2$	3.6×10^{-6} cm^3/s	[26]
65	$N_3^++e \rightarrow N_2(B^3)+N$	10^{-10} cm^3/s	[26]
66	$N_2(A^3)+e \rightarrow N_2+\check{e}$		
67	$N_2(B^2)+e \rightarrow N_2+\check{e}$		
68	$N_2^+(B^2)+e \rightarrow N_2$		
69	$N_2^+(C^2)+e \rightarrow N_2$		
70	$N_2^+(X^2)+e \rightarrow N_2$	Coefficients have been calculated according to formula (2)	
71	$N_2(C^3)+e \rightarrow N_2+\check{e}$		
72	$N_2^+(A^2)+e \rightarrow N_2$		
73	$N_2(a'^1)+e \rightarrow N_2+\check{e}$		
74	$N_2(a^1)+e \rightarrow N_2+\check{e}$		

2.3. Characteristics of the electric circuit

One of many methods of supplying the energy to an active medium and simultaneously the one most widely applied in nitrogen lasers is pumping by a lateral electric discharge [1]−[6]. The popularity of this method is caused by a relatively low costs of the supplying systems and their exploitation. These systems are characterized by small sizes, high reliability and the possibility of achieving high energetic efficiency. In the known theoretical models of the nitrogen laser, the electric charging systems are neglected due to significantly longer charging time of battery and condensers as compared to that of lasing action. The present model was constructed in a similar way. The electric circuit presented in Fig. 4a was accepted. It is a system of distributed-constant type operating on the principle of creating a travelling discharge wave along the channel formed by the electrodes [31]. For the rapid courses it can be approximated by the scheme shown in Fig. 4b. The distribution capacities C_L and C_R have been replaced by elements of Π-type (capacity−inductance−capacity). Such an approximation is sufficient for this model, since generation of laser radiation by the whole excited volume in this time has been assumed (see Sect. 4). On the other hand, the accepted scheme of the electric circuit truly renders the time dependences from the moment of short-circuiting in the spark-
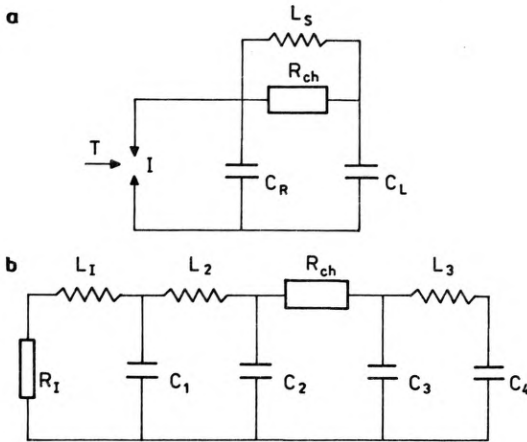
Fig. 4. Scheme of electric circuit for nitrogen laser (a) and scheme for rapid transitions (b). $R_{I,ch}$ — time variable resistance of commutator and chamber of the laser, respectively, $C_{L,R}$ — capacities, $L_{1,2,3}$ — inductance of spark gap, left plate and right plate (and the connectors), $C_{1,2,3,4}$ —componet capacities of the left and right plates

gap to the ending moment of the lasing action. In the chosen system, the circuit of preionization is an integral part of the main electric circuit. Thanks to such design the the initiation of the laser operation is done by one commutating element. Plane condensers distributed on both sides of electrodes are charged to a high voltage of order of serveral thousands of kilovolts. After triggering of the commutator I a difference of potentials occurs between the laser electrodes which evokes a fast increasing electric discharge across the active medium. After having reached the breakdown threshold the glow-discharge appears between the electrodes in the chamber. This circuit may be well described by a system of equations according to Kirchhoff laws. The respective equations for a substitute circuit for the nitrogen laser have the forms:

$$\frac{dI_I}{dt} = \frac{U_1 - I_I R_I}{L_I}, \tag{18}$$

$$\frac{dI_2}{dt} = \frac{U_2 - U_1}{L_2}, \tag{19}$$

$$\frac{dI_3}{dt} = \frac{U_4 - U_3}{L_3}, \tag{20}$$

$$\frac{dU_1}{dt} = \frac{I_2 - I_I}{C_1}, \tag{21}$$

$$\frac{dU_2}{dt} = \frac{I_{ch} - I_2}{C_2}, \tag{22}$$

$$\frac{dU_3}{dt} = \frac{I_3 - I_{ch}}{C_3}, \tag{23}$$

$$\frac{dU_4}{dt} = -\frac{I_3}{C_4}, \tag{24}$$

$$I_{ch}R_{ch} + U_2 = U_3. \tag{25}$$

The initial conditions for $t = 0$ are:

$$U_1 = U_2 = U_3 = U_4 = U_s, \quad I_1 = I_2 = I_3 = I_{ch} = 0. \tag{26}$$

Parameters R_I and R_{ch} appearing in the above equations describe the time-dependent resistances of the commutator and the chamber. Nonlinear resistance of the sparking discharge in the commutator R_I has been approximated with a semiempiric formula presented in papers [32], [33] describing the time-dependent resitsance in the sparking discharge

$$R_I = C_\beta d\rho^{1/3}\left[\int_0^t I_I^{2/3} dt\right]^{-1} \tag{27}$$

where: d — distance between the electrodes in commutator,

$\quad \rho$ — gas density in commutator,

$\quad C_\beta$ — experimental constant.

The presented way of describing the time-dependent resistance of commutator is an attempt to provide a more rigorous description of behaviour of this part of the circuit compared with the up-to-date applied models of numerical simulation of the nitrogen lasers. The resistance of commutator was presented by many authors of the laser models as a magnitude constant in time [10]

$$R_I = \begin{cases} \infty & t < 0 \\ R_0 & t \geqslant 0 \end{cases} \tag{28}$$

where typical value of $R_0 \approx 2\ \Omega$.

More accurate description of the behaviour of nonlinear time-dependent resistances has been applied in [15]

$$R_I(t) = R_0/[1 - \exp(-t/\tau)] \tag{29}$$

where $\tau = 1$–10 ns. The time τ is selected, depending on the value of the charging voltage.

Due to wide range of nonlinear resistance R_I and a large range of the time constants characteristic of the system (from 10^{-17} s to 10^{-7} s) the formula for R_I in the differential form has been added to the set of equations for the circuit. The dependence

$$R_{ch} = \frac{D_{ck}}{A_{ch}\mu e N_E} \tag{30}$$

where: D_{ch}, A_{ch} — distance and the front area of the electrodes in the chamber,

$\quad e$ — electron charge,

$\quad \mu$ — mobility of electrons,

has been applied to the description of main discharge resistance in the laser chamber, similarly as it was the case in the papers cited above.

The set of differential equations describing the electric circuit is conjugated with the kinetic equations by the change of the values of N_E and μ in time. In a complete theoretical model, the kinetic equations together with the equation for the energy of electrons and equations of the circuit must be completed by the radiation equation. The last one will be presented in the next subsection.

2.4. Equation of radiation

The radiation of a laser affects rather weakly the parameters of the medium plasma [34], hence in the description of kinetics of the laser medium some simplified expression for the time evolution of photon concentration in the resonator has been accepted . Namely, existence of only two states in the N_2 molecule has been accepted: the upper and lower laser levels. The density of photons N_F in the laser chamber has been thus described by the following equation:

$$\frac{dN_F}{dt} = A\frac{N_C}{\tau_s} + \frac{N_F c}{L_r}\left[(N_C - N_B)l_G\sigma - 0.5\ln\frac{1}{R_1 R_2} - l_G\Sigma N_i\sigma_i + \ln(1 - L_s)\right] \qquad (31)$$

where: N_F — concentration of photons of energy $E = hv_L$ (h — Planck constant),
$\quad\quad c$ — light velocity,
$\quad\quad N_C$, N_B — concentrations of respective laser states,
$\quad\quad \tau_s$ — delay time of the light intensity emitted spontaneously after stopping
$\quad\quad\quad\quad$ the excitation,
$\quad\quad \sigma$ — cross-section for the stimulated emission,
$\quad\quad L_r$ — length of resonator,
$\quad\quad R_1$, R_2 — coefficients of reflection of the resonator mirrors,
$\quad\quad N_i$ — concentration of particles absorbing the laser radiation,
$\quad\quad \sigma_i$ — cross-section for radiation absorption by i-th particle,
$\quad\quad L_s$ — medium losses,
$\quad\quad A$ — part of the spontaneous emission subject to amplification,
$\quad\quad l_G$ — length of the active medium.

Approximate power density of the laser radiation emitted by the resonator may be then determined as follows:

$$I_F = 0.5\ N_F chv_L \ln\frac{1}{R_1 R_2}. \qquad (32)$$

The equation for photon concentration evolution completes the set of equations of the theoretical model. The set of equations ((9), (11)) taking account of (18)−(25), (31) and the expresions (2), (12)−(17), (26), (30), (32) have been solved numerically using the subroutine FCN contained in the library procedure DGEAR (elaborated in IMSL). This procedure has been deviced basing on Gear algorithm for the method of backward differentiating. The assumptions taken for calculations as well as the due simplifications will be discussed in Sect. 3.

3. Assumptions for computations

The constructed theoretical model should be absolutely useful for simulations of

experimental examinations. Hence, in order to obtain the possibly highest number of laser characteristics as a function of many parameters, the necessary approximations should be done in the description of physics of N_2 laser pumped with electric discharge. The approximations have been introduced only to such parts of reasoning where the results did not differ from the accurate description, while they could be obtained much quicker.

The following simplifications have been made:

— uniformity of the active medium during the electric discharge,

— Maxwell type electron velocity distribution,

— mutual overlap of cross-sections of the radiation beam and the discharge region (rectangular cross-section),

— processes occurring at the main discharging electrodes of the laser chamber have not been taken into account.

A separate problem in the simulation of the nitrogen laser operation pumped by the electric discharge is how to determine the electron distribution function. In the case of nitrogen lasers pumped by electron beam, the Maxwell distribution is usually accepted [27], while for lasers pumped by electric discharge [1] an accurate electron distribution determined on the basis of the Boltzmann equation solution [35] according to the Rockwood model [36], [37] is used. The determination of the electron distribution function is necessary because the rates of reactions such as ionization, excitation and recombination depend on this function. Also the mobility of electrons as well as the rate of their elastic collisions (associated with the electron momentum transfer) with atoms and molecules are functions of electron distribution.

However, for majority of lasers based on electron transitions the assumption that the electron distribution suffers from thermalization in the time scale shorter as compared with other interesting processes [38] is correct. Hence, on the one hand, the error due to assumption of the Maxwell distribution, also in the case of lasers pumped by electric discharge, is not great, but on the other hand an accurate result can be achieved by means of solving the stationary Boltzmann equation. The solution of Boltzmann equation in the complete form being dependent also on time conjugated with kinetics is long-lasting and practically aimless. In the model presented in this paper, the Maxwell distribution of electron velocities was assumed. In the nitrogen lasers the electron density can be as high as $10^{14} - 10^{15}$ cm^{-3}. For such concentrations of electrons, the electron—electron collisions leading to the Maxwell distribution are essential. The characteristic time of those collisions can be estimated from the formula [28]

$$\tau_{EE} \approx \frac{m^{1/2} \varepsilon^{3/2}}{N_E e^4 \ln \Lambda} \tag{33}$$

where:

$$\ln \Lambda = \ln \left[\frac{3}{2\sqrt{\pi}} \frac{(kT)^{3/2}}{e^3 N_E^{1/2}} \right] \quad - \text{ Coulomb logarithm.}$$

For typical values of $N_E = 10^{14}$ cm^{-3}, $\varepsilon = 6-9$ eV, the characteristic time amounts

to $10^{-11}-10^{-10}$ s which is much shorter than the times characteristic of other processes, so that the "maxwellization" of electrons happens to follow each change of electron energy giving in consequence the Maxwell type electron velocity distribution at each moment of time. Thus, the assumption of the Maxwell distribution function for electrons

$$f(\varepsilon, \bar{\varepsilon}) = \frac{2\pi\varepsilon^{1/2}}{\left[\frac{2}{3}\pi\bar{\varepsilon}\right]^{3/2}} \exp\left[-\frac{3\varepsilon}{2\bar{\varepsilon}}\right] \tag{34}$$

being charged with a very small error within the range of accepted conditions shortens decisively the time of calculations allowing us to examine the influence of many external parameters on the nitrogen laser operation. Such a simplification allows us also to carry out the microcomputer calculations.

In the introductory analysis it has been established that the designed laser will be pumped by electric discharge with preionization by UV radiation. The theoretical model has been constructed in a way enabling achievement of maximal number of energetic characteristics of laser as functions of changing external parameters, such, for intance, as: supplying voltage as a function of definite parameters of laser chamber, sizes and shape and also the values of the electric circuit elements.

4. Summary

As the result of the analyses presented above a complete model of nitrogen laser excited by electric discharge was constructed. The kinetics of processes leading to achieving the needed population inversion of laser levels was elaborated. In the kinetic equations, over 70 reactions between the molecules and atoms have been described. Nonlinear resistance of commutator as well as preionization were taken into account when describing the electric circuit. The model description aimed to its maximal practical applicability, mainly to facilitate the design work on lasers. The obtained characteristics were used to design two models of nitrogen lasers of TEA type. The assumed simplifications (for instance, the assumption of the Maxwell distribution for electrons), while introducing a small error to the results of calculations, allowed us to carry out the microcomputer calculations, simultaneously shortening significantly the computing time. The results of the calculations carried out as well as their discussion will be presented in the paper [39].

References

[1] Kunabenchi R. S., Gorbal M. R., Savadatti M. I., Prog. Quantum Electron. 9 (1984), 259.
[2] Stankov K. A., Kurtev S. Z., Milev I. Y., Opt. Commun. 62 (1987), 29.
[3] Ibidem, p. 32.
[4] Saito Y., Nomura A., Kano T., J. Appl. Phys. 63 (1988), 2526.
[5] Papadopoulos A. D., Serafetinides A. A., IEEE J. Quantum Electron. 26 (1990), 177.
[6] Iwasaki Ch., Jitsuno T., IEEE J. Quantum Electron. 18 (1982), 423.
[7] Ali A. W., Kolb A. C., Anderson A. D., Appl. Opt. 6 (1967), 2115.

[8] DZAKOWIC G., KAN T., KUENNING R., SCHLIFT L., *Lawrence Livermore Laboratory Report*, UCID−16733, 1975.

[9] MORENO J. B., IEEE J. Quantum Electron. **14** (1976), 204.

[10] FITZSIMMONS W. A., ANDERSON L. W., RIEDHAUSER C. E., VRTILEK J. M., IEEE J. Quantum Electron. **12** (1976), 624.

[11] CHEN C. H., PAYNE M. G., HURST G. S., JUDISH J. P., J. Chem. Phys. **65** (1976), 3863.

[12] PUECH V., COLLIER F., COTTIN P., J. Chem. Phys. **67** (1977), 2887.

[13] GRIGORYAN YU. L, PAPANYAN V. O., *Issledovanie elektrorazryadnogo azotnogo lazera vysokogo davleniya*, Preprint IYUI-78-80, Erevan 1978 (in Russian).

[14] BRUNET H., VINCENT P., SERRA J. R., J. Appl. Phys. **54** (1983), 4951.

[15] SÁNTA L, KOZMA L., NÉMET B., HEBLING J., GORBAL M. R., IEEE J. Quantum Electron **22** (1986), 2174.

[16] GORSE C., CAPITELLI M., J. Appl. Phys. **62** (1987), 4072.

[17] DHALI S. K., LOW L. H., J. Appl. Phys. **64** (1988), 2917.

[18] HEARD H. G., Nature **200** (1963), 667.

[19] POKORA L., UJDA Z., [In] Int. Symp. *Laser'91*, Medical Congress, München, June 10−14, 1991, pap. 107.

[20] VELAZCO J. E., SETSER D. W., J. Chem. Phys. **62** (1975), 1990.

[21] POKORA L., KUTYLA J., WAWER J., SPIE **859** (1988), 112.

[22] LANDAU L. D., LIFSZYC E. M., *Mechanika kwantowa* (in Polish), [Ed.] PWN, Warszawa 1979.

[23] GUREWICZ D. B., KANATENKO M. A., PODMOSHENSKY I. V., Opt. Spektrosk. **54** (1983), 781.

[24] ANDERSSON H. E. B., BORGSTRÖM S. A., Opto-Electron. **6** (1974), 225.

[25] SUBHASH N., KARTHA S. C., SATHIANANDAN K., Appl. Opt. **22** (1983), 3612.

[26] HILL R. H., GUTSCHECK R. A., HUESTIS D. L., MUKHERJEE D. L., LORENTS D. C., Stanford Research Institute Report MP 74-39.

[27] JUDD O. P., IEEE J. Quantum Electron. **12** (1976), 78.

[28] SMITH K., THOMSON R. M., *Computer Modelling of Gas Lasers*, Plenum Press, New York 1978.

[29] MILLET P., SALAMERO Y., BRUNET H., J. Chem. Phys. **58** (1973), 5839.

[30] REGEMORTER VAN H., J. Astrophys. **136** (1962), 906.

[31] US Patent 4301425.

[32] BARANIK C. U., VASSERMAN C. B., LUKIN A. H., Zh. Tekh. Fiz. (in Russian) **44** (1974), 2352.

[33] HEER DE F. J., JANSEN R. H. J., J. Phys. B **10** (1977), 3741.

[34] STIELOW G., Appl. Phys. B **47** (1988), 333.

[35] FROST L. S., PHELPS A. V., Phys. Rev. **127** (1962), 1621.

[36] ROCKWOOD S. D., Phys. Rev. A **8** (1973), 2348.

[37] ROCKWOOD S. D., GREEN A. E., Comput. Phys. Commun. **19** (1980), 377.

[38] JOHNSON T. H., HUNTER A. M., J. Appl. Phys. **51** (1980), 2406.

[39] MAKUCHOWSKI J., POKORA L., Opt. Appl. **23** (1993), 131.